CONF-901025--6

CONF-901025--6

DE90 017326

SEP 1 8 1990

EDGE TURBULENCE AND TRANSPORT: TEXT AND ATF MODELING*

CH.P. RITZ, T.L. RHODES, H. LIN, W.L. ROWAN, R. BENGTSON, A.J. WOOTTON
Fusion Research Center, University of Texas
Austin, Texas 78712

B.A. CARRERAS, J.N. LEBOEUF, D.K. LEE, J. HARRIS, C. HIDALGO, J.D. BELL, J.A. HOLMES, R. ISLER, V.E. LYNCH, T. UCKAN
Oak Ridge National Laboratory
Oak Ridge, Tennessee 37831, U.S.A.

P.H. DIAMOND, A.S. WARE
University of California at San Diego
La Jolla, California 92093, U.S.A.

D.R. THAYER
Science Applications International Corporation
San Diego, California 92121, U.S.A.

DISCLAIMER

* Research sponsored by the Office of Fusion Energy, U.S. Department of Energy, under contract DE-AC05-84OR21400 with Martin Marietta Energy Systems, Inc.

EDGE TURBULENCE AND TRANSPORT: TEXT AND ATF MODELING

ABSTRACT

We present experimental results on edge turbulence and transport from the tokamak TEXT and the torsatron ATF. The measured electrostatic fluctuations can explain the edge transport of particles and energy. Certain drive (radiation) and stabilizing (velocity shear) terms are suggested by the results. The experimental fluctuation levels and spectral widths can be reproduced by considering the nonlinear evolution of the reduced MHD equations, incorporating a thermal drive from line radiation. In the tokamak limit (with toroidal electric field) the model corresponds to the resistivity gradient mode, while in the currentless torsatron or stellarator limit it corresponds to a thermally driven drift wave.

1. Introduction.

The motivation for studying the fluctuations and transport in the plasma edge is manifold; 1) experimental data exists which shows the electrostatic fluctuations explain the total transport, 2) theories are better developed than for the core, and 3) modeling can be performed mainly using fluid equations. In an attempt to understand the edge turbulence a comparative study of the currentless torsatron ATF and tokamak TEXT has been initiated. We start by describing results from TEXT, noting how experiment and theory have influenced each other. Next we present results from ATF, comparing them with those from TEXT. The final section provides both a historical perspective of the attempts to model the results, and a summary of the latest comparisons.

2. TEXT

Table 1 lists the edge equilibrium and fluctuating parameters for typical TEXT discharges [1], and Fig. 1 shows the radial dependence of the normalized density fluctuation level, $\tilde{n}/n$. The turbulence is broadband, with frequency width $\sigma_f \approx \bar{f} \approx 150$ kHz, and wave number (spectral) width $\sigma_{k\theta} \approx \bar{k}_\theta$. Typically $\bar{k}_\theta \approx 2$ to 3 cm^{-1}, so that $\bar{k}_\theta \approx 0.05$, and correlation lengths $\ell_\theta \approx 1$ cm, $\ell_r \approx 0.5$ cm. Typically $e\tilde{\phi}/T_e > \tilde{n}/n$ and $\tilde{T}_e/T_e < \tilde{n}/n$ are found. The small magnetic fluctuation level measured ($\tilde{b}/B_\phi \leq 10^{-5}$) at $r > a$ is well correlated with the measured $\tilde{n}$ at $r < a$, suggesting that $\tilde{b}$ is the result of a perturbed current density at $r < a$ [2].

The fluctuation levels are determined primarily by material probes. In the usual technique [3] the plasma potential ϕ and its fluctuation level are determined by assuming $\phi_{float} = \phi - \delta T_e$. Uncertainties in δ translate

directly to uncertainties in ϕ, T_e, $\tilde{\phi}$, and $\tilde{T}_e$. However, the important result that $(ne\tilde{\phi})/(T_e\tilde{n}) > 1$ is confirmed by a heavy ion beam probe.

Initial modeling [5] showed that resistivity gradient driven turbulence, rather than collisional drift waves which are stable due to the electron temperature gradient, could explain the measured correlation lengths (in Macrotor), and predicted fluctuation levels were ~10 to 15%. The result $(ne\tilde{\phi})/(T_e\tilde{n}) > 1$ motivated the inclusion of thermal and condensation drives for the resistivity gradient mode [6]. In turn, the modelling suggested that controlled impurity injection should be performed. Experiments with purposely added impurities in TEXT show that $e\tilde{\phi}/T_e$ can be strongly modified in the edge. Assuming the probe technique is unaffected by the impurities, N_2 puffing increases $\tilde{\phi}$ but not $\tilde{n}$ in regions where $T_e \approx 20$ ev. The electrostatic fluctuation driven flux Γ^f increases. The results suggest a thermal drive in the region where the cooling rate decreases with increasing T_e. Rapidly decreasing the applied toroidal electric field E_ϕ by 90% has no significant effect on the edge turbulence properties. The local parameters T, n, $\tilde{n}$, $\tilde{\phi}$, and $\tilde{b}$ remain practically unchanged for several confinement times. This excludes E_ϕ as the sole driving term, again suggesting that resistivity gradient driven turbulence is not a complete explanation for the observations.

The measured ensemble averages $\langle\tilde{n}\tilde{\phi}\rangle$ and $\langle\tilde{T}_e\tilde{\phi}\rangle$ account for the total particle and energy fluxes. Regression analysis of the electrostatic fluctuation driven flux Γ^f for $r \approx a$ shows the results are fit by $\Gamma^f \propto nB_\phi^{-2\pm1}$. The density gradient scale length L_n behind the single poloidal ring limiter is well fit by balancing Γ^f with flow at 0.5 c_s along field lines. The measured fluctuation amplitudes and correlations predict the measured ratio L_{Te}/L_n, but the result is very sensitive to the secondary electron coefficient which determines the parallel heat flux to the limiter.

While the equilibrium density and temperature fall smoothly with increasing minor radius, there is a mass velocity shear layer near the outermost closed flux surface (at $r = a$). Here the radial electric field E_r changes sign; the fluctuation phase velocity $v_{ph} \approx v_{de} - E_r/B_\phi \approx 0$ (v_{de} is the electron diamagnetic velocity) at the shear layer radius $r = a_s$. In this shear layer the turbulence correlation time in the rotating frame is reduced from $> 10\mu s$ to ≈ 1 to $3\mu s$, ℓ_r is reduced, and the fluctuation amplitudes reduced. These features are in agreement with theoretical predictions [7]. These radially localized effects can be displaced by purposely modifying E_r, either by using biased limiters or external windings to create a stochastic magnetic field. These results support the notion that a mass velocity shear is a strong stabilizing influence.

3. ATF

ATF is an $\ell = 2$, 12–field period torsatron with major radius $R = 2.10m$, average minor radius $\bar{a} = 0.27m$, magnetic field on axis $B \leq 2$ Tcentral rotational transform $\iota_0 = 1/q_0 \approx 0.3$, and edge transform $\iota_a = 1/q_a \approx 1$. Typical edge equilibrium and fluctuating parameters are

similar to TEXT, as seen from Table 1. The majority of ATF data for this study were taken at $B = 0.95\ T$ in currentless plasmas produced with 200 to 400kW of 53GHz second harmonic electron cyclotron heating (ECH) power. This explains the lower operating density.

Like TEXT, ATF has a shear layer where E_r and v_{ph} change sign. When the radial profiles of $\tilde{n}/n$ are plotted with the radius normalized to the radius of the shear layer, the resulting dependence is very similar to that seen in TEXT (Fig. 1). This suggests that the shear layer is the functional boundary of the plasma.

In ATF, the location of the shear layer shifts with the vacuum magnetic configuration when the externally imposed vertical field is varied. The shear layer also moves inward when the rail limiter (toroidal extent $\approx 9°$) is moved inside the nominal last closed magnetic surface where $\iota \approx 1$. The shear layer is also affected by the main plasma parameters: it moves radially outward by 2–3 cm as the plasma stored energy increases in both ECH and neutral beam injection heated plasmas.

As in TEXT, the $\tilde{n}$ and $\tilde{\phi}$ frequency spectra are broad, and dominated by fluctuations at frequencies < 200 kHz. The values of Γ^f are comparable to those estimated from global particle balance measurements [8]; as in TEXT Γ^f increases with increasing n at a fixed radius. The perpendicular wave number spectra are also broad, with $\sigma_k/\bar{k} = 0.5 - 1$. Figure 2 shows that $\sigma_{k\theta}(\propto 1/\ell_\theta)$ varies systematically with the poloidal phase velocity of the fluctuations both in TEXT and in ATF. In both machines a maximum value is reached at the shear layer itself (where $v_{ph} = 0$): typically, $\sigma_{k\theta}(\mathrm{ATF})/\sigma_{k\theta}(\mathrm{TEXT}) \approx [q_a(\mathrm{ATF})/q_a(\mathrm{TEXT})]^{-1}$, in accordance with expectations for fluctuations resonant with the pitch of the magnetic field.

Under some conditions a highly coherent peak is found [9] with probes and reflectometer at $f \approx 50$ kHz with $\ell_\theta \geq 2$ cm $\approx L_n$. While the fluctuation is large ($\tilde{n}/n \sim 10^{-2}$) it does not contribute appreciably ($\leq 10\%$) to Γ^f at the edge.

4. Modelling.

Modelling started with resistivity gradient driven turbulence [5]. Failure to account for $(ne\tilde{\phi})/(T_e\tilde{n}) > 1$ and $\sigma_{k\theta} \approx 2-3\ \mathrm{cm}^{-1}$, led to thermally driven convective cell turbulence [6], where the desired enhancement is provided by radiation through thermal and condensation [10] drives. We have since shown condensation to be not only unimportant but invalid [11]. Since TEXT and ATF results have shown that E_ϕ is not the important drive, we are investigating thermally driven drift waves [12] as limits of thermally driven convective cells when the loop voltage fades away and diamagnetic effects take over. The basic equations are Ohm's law,

$$\frac{\partial \psi}{\partial t} = -R\nabla_\parallel \tilde{\phi} + R\eta \tilde{J}_\parallel + R\frac{E_\phi}{\eta}\tilde{\eta} + R\tilde{\eta}\tilde{J}_\parallel - \frac{R}{B_\phi e}\alpha \nabla_\parallel \tilde{T} \qquad (1)$$

the moment :m balance equation,

$$\frac{\partial(\nabla_\perp^2\tilde{\phi})}{\partial t} + \vec{v}\cdot\vec{\nabla}(\nabla_\perp^2\tilde{\phi}) = -\frac{B_\phi^2}{\rho_m}\nabla_\parallel\tilde{J}_\parallel + \mu\nabla_\perp^2(\nabla_\perp^2\tilde{\phi}) \qquad (2)$$

the electron temperature equation,

$$\frac{\partial\tilde{T}}{\partial t} + \vec{v}\cdot\vec{\nabla}\tilde{T} = \chi_\parallel\nabla_\parallel^2\tilde{T} - \tilde{v}_r\frac{dT_e}{dr} + \gamma_R\tilde{T} + \chi_\perp\nabla_\perp^2\tilde{T} + \frac{2/3\alpha}{B_\phi en}T_e\nabla_\parallel\tilde{J}_\parallel \qquad (3)$$

Here η denotes the resistivity, μ the viscosity, $\chi_\parallel$ and $\chi_\perp$ the parallel and perpendicular thermal conductivities, and $J_\parallel$ the parallel current. The radiation drive $\gamma_R = -2/3n_z dI_z(T_e)/dT_e$, where n_z is the impurity density and the intensity of the cooling is given by $I_z(T_e)$.

Analytical theory [12] shows that the turbulence saturation condition is the result of the enhanced parallel diffusion by the radial turbulent transport balancing the resistivity gradient (when $E_\phi \neq 0$) and/or thermal instability drives. The predicted potential saturation level, in the radiation dominated regime, can be expressed as

$$\frac{e\phi}{T_e} = \frac{\gamma_R^{3/2}(1+2/3\alpha^2)}{(\chi_\parallel k_\parallel'^2)\bar{k}_\theta\rho_S C_S} \qquad (4)$$

where $k_\parallel' = \bar{k}_\theta/L_s$, and $\alpha = 1.71$ for thermal drift waves or $\alpha = 0$ for resistivity gradient driven turbulence.

The computations are performed in cylindrical geometry using our 3D nonlinear, initial value, reduced MHD code KITE [13]. They are carried out with TEXT edge parameters and profiles in a region where $q \approx 2.8$, $T_e \approx 15$ eV, $n \approx 4.5\times10^{12}$ cm^{-3} and $n_z \approx 8.0\times10^{10}$cm^{-3}. The radiation function $I_z(T_e)$ is based on a shifted coronal equilibrium. While the model $I_z(T_e)$ is in agreement with TEXT bolometric data, recent TEXT and ATF measurements indicate that the radiated power for a single line is peaked at smaller radii than we have used. This discrepancy suggests not only that the choice of the functions $I_z(T_e)$, $n_z(r)$ and $Z_{\rm eff}(r)$ are critical to the results, but other drives such as ionization (an electron thermal energy sink and density drive) and charge exchange (momentum and ion thermal sink).

Nonlinear calculations in the resistivity gradient driven turbulence limit with radiation drive, applicable to Ohmic TEXT discharges, show that the fluctuation levels are in good agreement with the theoretical predictions. They are also in reasonable agreement with experimental measurements at the edge of TEXT in both their magnitude and radial distribution. Figure 3a shows $e\tilde{\phi}/T_e$ (most accurately modelled, although $\tilde{n}/n$ is the most accurately measured) from the experiment, computation and analytic theory (Eq. (4)). The model can explain both the measured $e\tilde{\phi}/T_e > 40\%$, and the measured $e\tilde{\phi}/T_e > \tilde{n}/n$. It yields a magnetic fluctuations level 5 times higher than the experiment but with a radial dependence consistent with the experimental one.

The calculated $\sigma_{k\theta}$ values range from 1 to 2 cm^{-1} as compared to experimental values of 2 to 3 cm^{-1}. The calculations show there is a strong dependence of $\sigma_{k\theta} \approx \bar{k}_\theta$ on radius, therefore on the q profile, with $\sigma_{k\theta}$ scaling as q in a radially averaged sense. Since $q_a \sim 3$ in TEXT and $q_a \sim 1$ in ATF, we predict $\sigma_{k\theta}$ for ATF to be about a factor of 3 lower than for TEXT. This was confirmed in Fig. 2.

The calculations also yield $\tilde{T}_e/T_e \geq \tilde{n}/n$. This result has been confirmed theoretically [11] and agrees with preliminary upper estimates in ATF with $r < a_s$, but disagrees with TEXT measurements which were performed for $r > a$ where the model may be invalid. Calculations in the thermally driven drift wave limit, applicable to edge current free TEXT discharges and the currentless ATF, have also been performed with TEXT parameters. Thermal drift waves are stabilized by electron temperature gradients. Instability with growth rates comparable with the rippling mode with radiation drive growth rates can be recovered using the experimental radiation strength ($I_z(T_e)$ amplitude). As illustrated in Fig. 3b, saturation levels of $e\tilde{\phi}/T_e \approx 50\%$, comparable to those obtained with the resistivity gradient turbulence with radiation drive, can be achieved. The calculations also yield $\sigma_{k\theta}$ values between 0.75 and 1.5 cm^{-1}. These results might explain the similarities observed between TEXT with $E_\phi \neq 0$ (resistivity gradient with radiation?), TEXT with $E_\phi \approx 0$ (thermal drift wave?), and ATF (thermal drift wave?). An important feature of the calculations is the self-generation, through the nonlinear couplings between unstable propagating modes, of a *dc* potential and hence of a sheared electric field by the drift wave turbulence. This *dc* potential helps saturate the instability and quench the turbulence.

Ongoing work includes 1) obtaining and using more realistic estimates $I_z(T_e)$, $n_z(r)$, and $Z_{eff}(r)$, 2) applying the thermal drift wave model to ATF parameters, 3) the incorporation of the ionization term in the rippling plus radiation model, 4) the inclusion of the ionization and radiation terms in the collisional drift wave model, and 5) the inclusion of limiter effects. The importance of ionization is already recognized; it destabilizes the collisional drift wave and provides a purely inward particle flux, offering a candidate to explain the inward pinch term required in tokamak modeling. In the future all the above aspects will be incorporated in a single model.

Work supported by the U.S. Department of Energy.

REFERENCES

[1] RITZ, CH.P., BROWER, D.L., RHODES, T.L., BENGTSON, R.D., et al., *Nucl. Fusion* **27**, (1987) 1125.

[2] KIM, Y.J., GENTLE, K.W., RITZ, C.P., RHODES, T.L., and BENGTSON, R.D., *Nucl. Fusion* **29**, (1989) 99.

[3] RITZ, CH.P., POWERS, E.J., RHODES, T.L., BENGTSON, R.D., et al., *Rev. Sci. Instrum.* **9**, (1988) 1739.

[4] ROBINSON, D.C., and RUSBRIDGE, M.G., *Plasma Physics* **11**, (1969) 73.

[5] GARCIA, L., DIAMOND, P.H., CARRERAS, B., and CALLEN, J., *Phys. Fluids* **28** (1985) 2147; HAHM, S., DIAMOND, P.H.,

TERRY, P.W., GARCIA, L., CARRERAS, B.A., *Phys. Fluids* **30**, (1987) 1452.
[6] THAYER, D.R., AND DIAMOND, P.H., *Phys. Fluids* **30**, (1987) 3724.
[7] CHIUEH, T., TERRY, P.W., DIAMOND, P.H., and SEDLAK, J.E., *Phys. Fluids* **29**, (1986) 231; BIGLARI, H., et al., IAEA-CN-53/D-3-5-3, this meeting.
[8] UCKAN, T., BELL, J.D., HARRIS, J.H., CARRERAS, B.A., DUNLAP, J.L., DYER, G.R., RITZ, CH.P., WOOTTON, A.J., RHODES, T.L., and CARTER, K., *J. Nucl. Mater.* accepted for publication (1990).
[9] HARRIS, J., et al., IAEA-CN-53/C-4-7, this meeting.
[10] DRAKE, J.F., *Phys. Fluids* **30**, (1987) 2429.
[11] THAYER, D.R., and DIAMOND, P.H., SAIC Technical Report #SAIC-90/1207:APPAT-130, SAIC, La Jolla, CA, (1990).
[12] WARE, A.S., DIAMOND, P.H., THAYER, D.R., CARRERAS, B.A., and LEBOEUF, J.N., Paper 1C13, 1990 Sherwood Theory Conference, Williamsburg, VA, April 23-25, (1990).
[13] GARCIA, L., HICKS, H.R., CARRERAS, B.A., CHARLTON, L.A., and HOLMES, J.A., *Journ. Comp. Phys.* **65**, (1986) 253.

Table I. Equilibrium and turbulence characteristics

	TEXT	ATF	Resistivity Gradient Limit	Drift Wave Limit
B_ϕ	2T	1T		
$n(cm^{-3})$	4×10^{-12}	1×10^{-12}		
$T_e(ev)$	30	20		
q	3	1		
$\tilde{n}/n$	$0.1 - 0.2$	$0.05 - 0.1$	0.1	
$\tilde{T}_e/T_e$	$0.05 - 0.1$ (for $r > a$)	0.1 (upper limit)	0.2	0.3
$\tilde{\phi}/T_e$	$0.15 - 0.3$	$0.1 - 0.2$	0.4	0.5
$\sigma_{k\theta}(cm^{-1})$	3	1	$1 - 2$	$0.75 - 1.5$

FIGURE CAPTIONS

Fig. 1. The radial dependence of normalized density fluctuation levels. The radial coordinate is normalized to the minor radius a_s of the shear layer itself. Results for TEXT (solid triangles) and ATF (open circles) are shown.

Fig. 2. The radial dependence of the width $\sigma_{k\theta}$ of the fluctuation k_θ spectrum. The radial coordinate is normalized to the shear layer minor radius a_s. Results for TEXT (open circles) and ATF (solid squares) are shown.

Fig. 3. Radial dependence of normalized potential fluctuation levels measured and predicted for TEXT. 3a) resistivity gradient driven model with radiation: experiment (solid circles), analytic theory (solid squares) and computational model (open squares) values. 3b) thermally driven drift wave model: resistivity gradient with radiation (open squares) and thermal drift wave (solid triangles) computational model values .

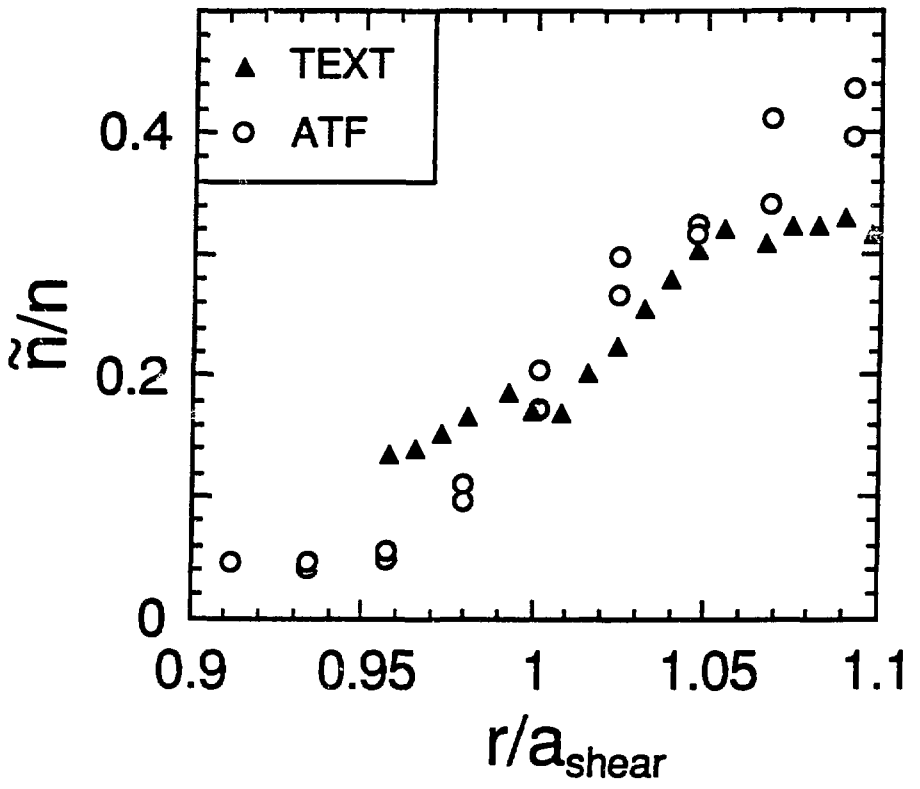

Fig. 1

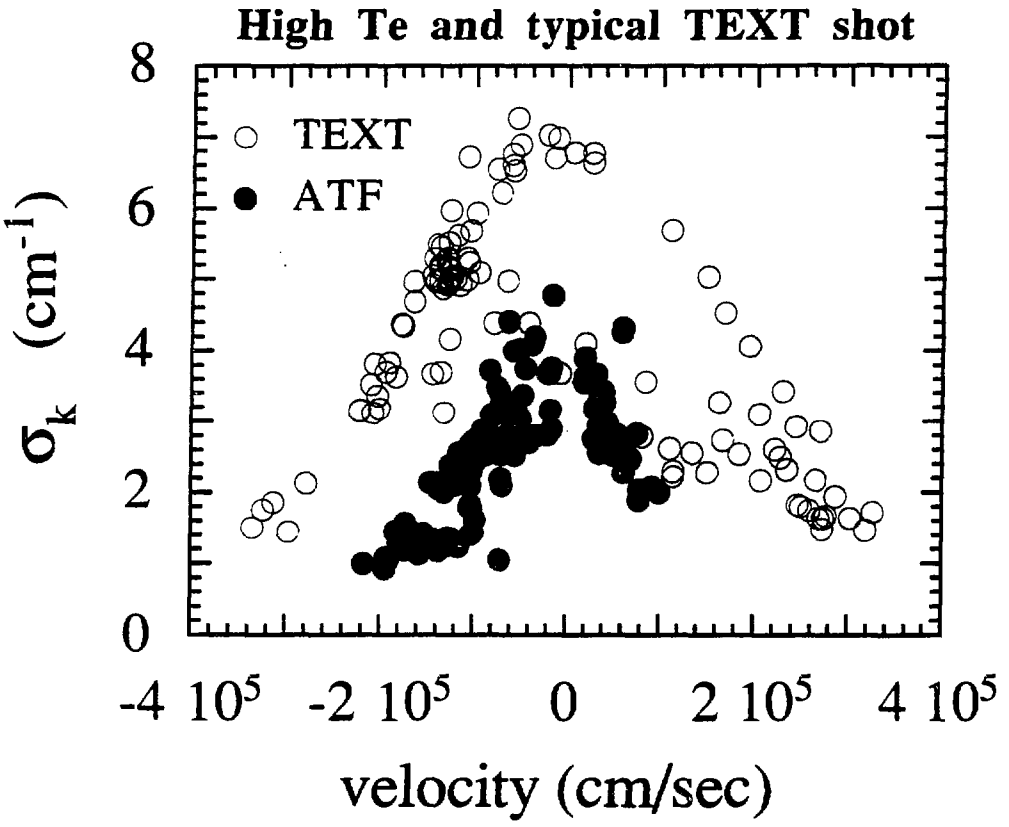
High Te and typical TEXT shot
TEXT
ATF
8
6
4
2
0
σ_k (cm^{-1})
-4 10^5
-2 10^5
0
2 10^5
4 10^5
velocity (cm/sec)

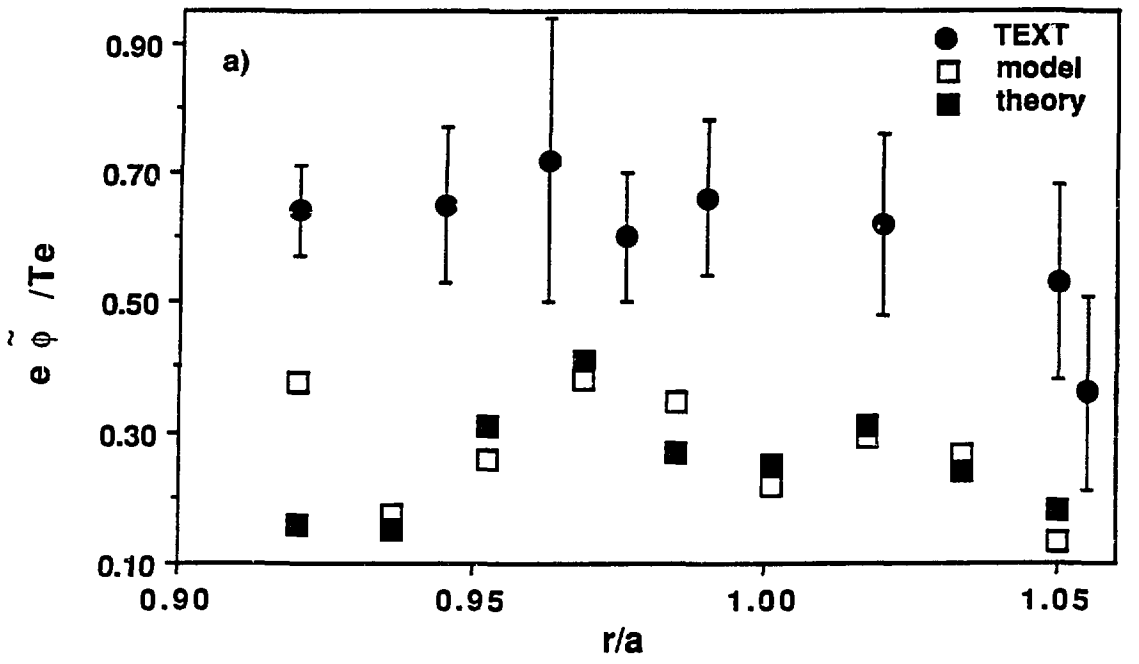
a)
TEXT
model
theory
0.90
0.70
0.50
0.30
0.10
0.90
0.95
1.00
1.05
r/a
e φ /Te

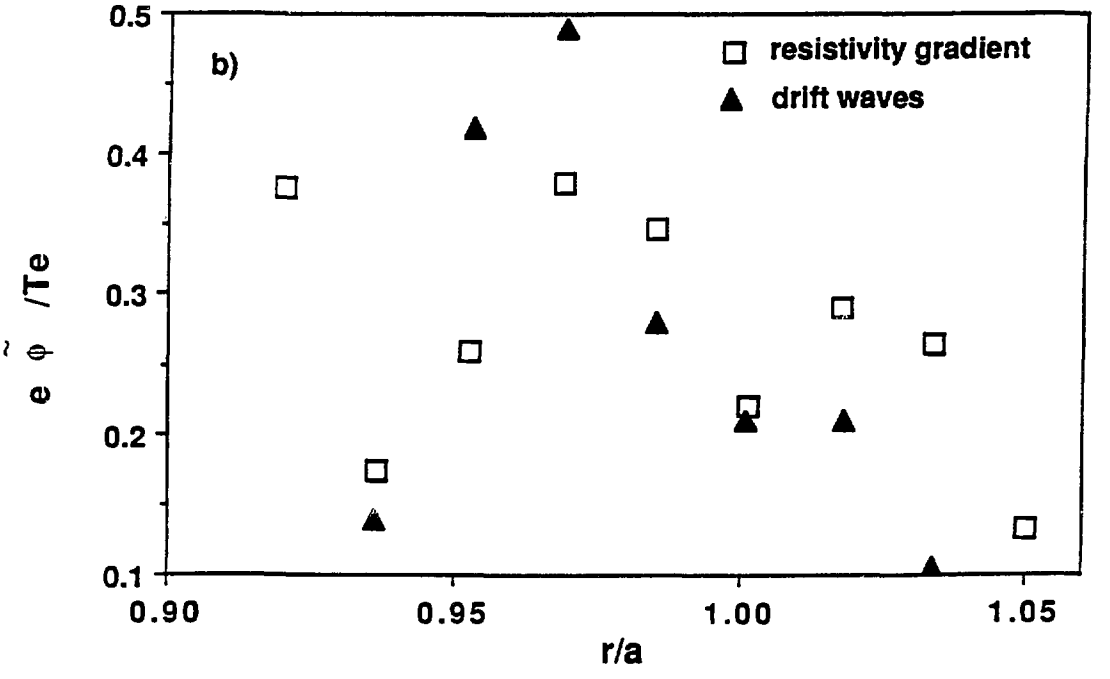
b)
resistivity gradient
drift waves
0.5
0.4
0.3
0.2
0.1
0.90
0.95
1.00
1.05
r/a
e φ /Te